



Original Research Article

A Novel Approach to Stop the Fire Spread, Hazardous Gases and Radionuclides

Abykanova B.^{1*}, Karatayeva K.², Shazhdekeyeva N.², Suleimenova B.³, Bekova G.⁴, Kochshanova G.⁵, Yerekeshova A.⁶, Urazgaliyeva M.⁶

¹Candidate of Pedagogical Sciences, Kh. Dosmukhamedov Atyrau University, Atyrau, Kazakhstan

²Candidate of Physical and Mathematical Sciences, Kh. Dosmukhamedov Atyrau University, Atyrau, Kazakhstan

³Master of Science in Natural Sciences, Docent Atyrau, University of Oil and Gas Named After Safi Utebayev, Atyrau, Kazakhstan

⁴Master of Natural Sciences, Atyrau University, Atyrau, Kazakhstan

⁵Candidate of Pedagogical Sciences, Caspian University of Technology and Engineering Named After Sh. Esenova, Aktau, Kazakhstan

⁶Senior Lecturer, Atyrau, University of Oil and Gas Named After Safi Utebayev, Atyrau, Kazakhstan

ARTICLE INFO

Article history

Submitted: 2020-11-07

Revised: 2020-11-25

Accepted: 2020-12-01

Manuscript ID: CHEMM-2011-1306

DOI: [10.22034/chemm.2021.122287](https://doi.org/10.22034/chemm.2021.122287)

KEYWORDS

Fire Spread

Nuclear power plants

Sogda

Water film

ABSTRACT

In the current study, we attempted to introduce a novel approach to stop the fire spread in all type of fires and improve the fire and explosion safety for LNG storage. In so doing, we relied on the application of innovative technology "Sogda". The design of a screen "Sogda" consists of two parallel metallic grids stretched over metallic frames. Active special water spray nozzles located between two parallel fixed grids creates water film on the surface of grid and water vapor droplet-air medium in the space between two parallel grids. This complex process partially attenuates the radiant heat flow from 45 to 100 kW/m^2 or more times, representing mainly in electromagnetic waves in an IR diapason, as a result of thermo-physical effects and it is optical phenomena that prevent the passage of explosive, toxic gases.

GRAPHICAL ABSTRACT

The application of innovative technology "Sogda"



* Corresponding author: Abykanova B.

✉ E-mail: education.com.kz@gmail.com

© 2020 by SPC (Sami Publishing Company)

Introduction

A firefighter is a worker whose primary function is to respond to emergencies in several different places to save lives, rescue and mitigate property damage. The role of protective clothing and other personal protective equipment (PPE) is fundamental to the safety of firefighters as they combine the need for life and property with protection in complex and increasingly diverse alarm situations. Preparedness for reaction and prevention are also critical aspects of this work. Firefighters responding to a fire call may now notice that chemical and biological toxins are also exposed to them. In the 20th century addressing the issues related to thermal protection of firefighters and reduction/prevention of fire spread has witnessed significant progress [1–10].

As a fire barrier, partitions made of concrete and various heat shields are generally used to form fire-resisting walls and fire compartments. Thermal Protective Equipment/Aides have also been used for thermal protection of firefighters, known as fire-fighter clothing, manual forming of water curtains etc. and their function is based on the fact that they reflect or absorb radiant energy. However, previously used TPA's or fire barriers have a number of disadvantages: Firewalls and partitions have limited fire resistance, they are much heavier building in terms of construction and structure, forming water curtains requires a lot of water discharge, thermal protective clothing of firefighters is not adequate to effectively attenuate the radiant heat flux and it has significant limitations on the time of use when exposed under high heat flow [11–14]. Despite this, the researchers' attention has been drawn to work on universal protective heat shields and their materials [15–18].

In the current study, as a novel strategy, the focus of the research was upon breakthrough solutions to address the above-mentioned deficiencies. Obviously, working in this area requires a thorough theoretical and experimental study of the physical processes of the interaction of thermal radiation with different kinds of

materials, inclusive of their possible compositions and designs.

Heat Protective Fence

Nowadays, cumulated experience in the use of screen "Sogda" as an active means of fire protection in fires gives the inspiration to implement local protection into practice for isolated LNG storage facilities [3–15]. The screen is used to shield firefighters who, in the process of extinguishing the oil and gas gushers, handle the portable fire-fighting hoses. These hoses are set up near the gusher's mouth. The echelon safety of firemen is widely used because the strength of heat radiation from the gusher is very high. This form of defence is arranged by positioning some firemen in the direction of the gusher and at some intervals with manual fire-fighting hoses.

The design of a screen "Sogda" consists of two parallel metallic grids stretched over metallic frames [19]. Active special water spray nozzles located between two parallel fixed grids creates water film on the surface of grid and water vapour droplet-air medium in the space between two parallel grids. This multi-phase complex process partially absorbs the radiant heat flow reflecting electromagnetic waves mainly in an infrared diapason and prevents the passage of explosive, toxic gases as a result of thermo-physical effects, and it is an optical phenomenon [20–22].

In the absence of water supply in the system, the fence provides visibility-allowing air and gas passage through that provides natural ventilation [23,24]. Furthermore, even after prolonged use of this fence against minor gas leaks, it will not lead to the accumulation of hazardous gas concentration inside the enclosure.

In case of emergency gas leakage or a fire, the space between two grids becomes a droplet-air environment due to automatically activated water spray nozzles within the grids and creates continuous water film impermeable for air and gas flows. Furthermore, in case of a fire, the thermal and optical phenomena occurring as a

result of the interaction of heat flow with the grid surface while water droplets distribution within grids creates water films on the grids attenuating the heat flow 50 times or more.

Overview of experiment

Background of experiment

The design of a highly effective protective screen was based on the aforementioned method of reducing the radiant heat flow and features such as properties, design optimization, performance and quality of the screen. The main tasks of optimizing the screen design are to ensure:

- Optimal reduction of radiant heat flux;
- Reliability and it is service life;
- Optimum water discharge;
- Technological design and it is optimal weight;
- Optimum visibility through screen;

The test specimen was appointed comprising the following items: A source of heat flow of up to 25

kW/m^2 , the mobile platform with the integrated protective screen, the water supply and measurement system etc. (Figure 1). The module of protective heat screen consisted of two metal mesh surfaces (area $-1m \times 1m$, fixed parallel to each other supported by a structural framework. Various materials for the protective screen were tested with various mesh sizes, including nozzle replacements. The assessment of the screen performance also included the change of a gap between grids and the distance from the source of heat flow to the screen. The water flow rate of $0.02 - 0.2 l/s$ was used for the nozzle at pressure up to $1 MPa$, providing a measurement of heat flow in the range of $0.05 - 25 kW/m^2$ with an accuracy variance of $0.01 kW/m^2$. The specially designed thermocouples are used to measure the temperature of the water film on the screen surface in the range of $0\text{ }^{\circ}C - 100\text{ }^{\circ}C$ with an accuracy of $0.10\text{ }^{\circ}C$.

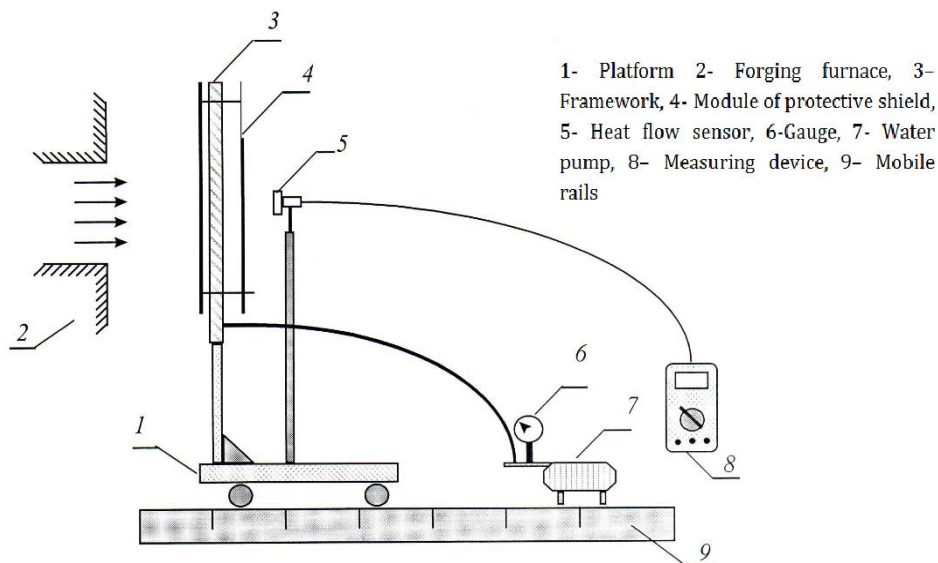


Figure 1: The overall configuration of the test specimen

The particular type of nozzle was developed to provide optimal water spray within the geometry. The water flow rate was determined by the diameter of the nozzle jet $-d$ and the pressure supply at the discharge point. The diameter and the statistical distribution of droplets were carried out on a special testing facility (Figure 2) and were used for further theoretical calculations. On a horizontal plane of

100 cm beneath the axis of the spray nozzle, the identical glasses were placed every 20 cm equally within the screen surface. The droplet diameter was determined via an arranged microscope. As a substrate for precipitating water droplets, the glass plate of 10×15 cm with the non-wetting surface was used. It was covered with a layer of technical oil forming a thickness of $2/3$ microns. The plates were held horizontally

over these glasses for one second. Therefore, the main parameters were water flow rate $-Q$, which appeared as droplets whilst travelling from the nozzle to the make contact with the screen

within the space between two grids and the distance between grids $-h$, and these factors defined the properties affecting the degree of attenuation of the heat flow.

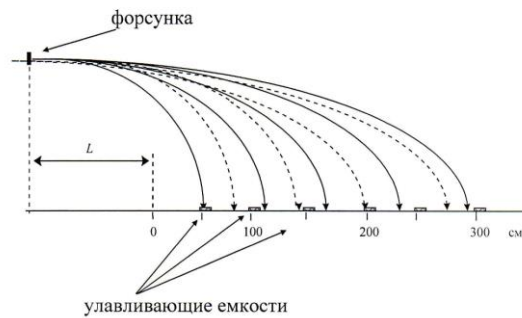


Figure 2: Illustration of a method that determines the statistical distribution of droplets with various diameters produced by the nozzle

This is an overview of the results of the most typical experiment when the maximum radiant heat flux of $P_0 = 25 \text{ kW/m}^2$ was exposed to screen. The screen performance was recorded comprising the following parameters: Water spray nozzle at the flow rate of 38 g/s, 65 g/s and 80 g/s operated at the pressure of 0.6 MPa. The distance between grids $-h$, was recorded at values equal to 5, 10, 15 and 20 cm for each nozzle. Visual observation indicated the following when the water flow rate was recorded:

- At 38 g/s, it collided with the heated grids, partly reflecting and breaking into smaller droplets to evaporate.
- At 65 g/s, these processes were accompanied by water film formation that appears on the surface of the individual grid.
- At 80 g/s, it led to an almost abrupt formation of complex water film on the surface of the grids. It was due to the process of multiple reflections of droplets that determined the direction and magnitude of the momentum vector of each droplet at the specified distance between the grids $-h$.

The attenuation coefficient of radiant heat flux $-K$ was derived for each experiment and plotted against the specified distance between the grids $-$

h , as shown in Figure 3. The attenuation coefficient of radiant heat flux $-K$ is defined as:

$$K = P_0/P \quad (1)$$

Where P_0 and P are respectively the values of the radiant heat flux exposed on the screen and heat flow passing through it.

The summary of measurements for an attenuation coefficient $-K$, at various distances $-R$, between the screen and radiant heat source is shown in Table 1. The optimum value for the distance between grids $h=15 \text{ cm}$ was used to determine the screen performance.

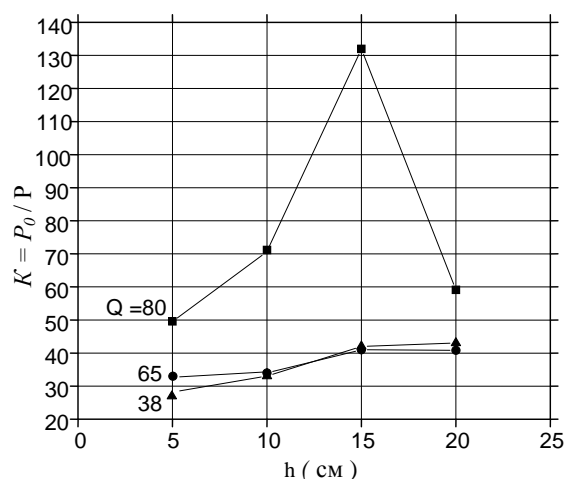


Figure 3: The attenuation coefficient of heat flux is as a function of h -distance between grids and Q -water discharge. Water flow rate is indicated next to each curve

Table 1: Attenuation coefficient -K is a function of a distance R between the screen and radiant heat source

Water flow rate <i>Q, g/s</i>	Distance between the screen and radiant heat source -R, cm			
	75 cm	125 cm	175 cm	225 cm
	Attenuation coefficient -K			
38	40	37	35	37
80	130	175	285	310

At the distance $R= 5\text{ cm}$, the temperature of the water film on the 1st front surface of the grid indicated $T=85\text{ }^\circ\text{C}$ at the given radiant heat flow of 25 kW/m^2 and decreased to $17\text{ }^\circ\text{C}$ when the screen was placed at the distance $R= 255\text{ cm}$. The corresponding temperature of the water film on the 2nd surface of the screen at distance $R= 75\text{ cm}$ also reduced from $21\text{ }^\circ\text{C}$ to $15\text{ }^\circ\text{C}$ when the screen was moved away at a distance 125 cm from the heat source.

Result and Dissection

This report was an analysis of the performance of screen “Sogda”. The experiment showed how the process of absorption and reflection of radiant heat flow could be calculated to address the qualitative physical explanation based on the theoretical model.

The simplified model of the screen as shown in Figure 4 mainly consists of two metallic grids -I and -III, length and height equal to $-l$ and located at a distance $-h$ from each other. In the space between the grids of the screen, is a water spray nozzle -II that provides water droplets. In order to construct a qualitative theoretical model, the following assumptions are required:

- Phenomena occurring on each structural element of the system are affected by time;
- Structural elements are in constant radiant and convective heat transfer to each other. It should be noted that the energy of combustion is transferred to the environment, mainly through the electromagnetic waves of radiant flame. In this case, the flame temperature of burning substances does not exceed $1100\text{ }^\circ\text{C} - 1800\text{ }^\circ\text{C}$, according to the theory of optical radiation. The part of radiant energy of fire uses the infrared

field of the electromagnetic waves (IR spectrum) with wavelengths much longer wavelengths of the visible spectrum.

Absorption and scattering of the radiation intensity $-P_0$, in the form of a metal mesh initially depends on the ratio of the area of metal parts to the total area of the grid $-\alpha_0$. To simplify the calculations, we assumed that the coefficient $\alpha_0 = 0.5$. The emissivity of such a network without cooling it with water would be equal to as 0.5 (Figure 4) [25].

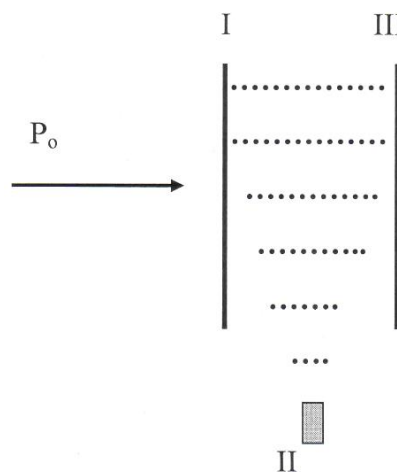


Figure 4: Schematic view of the heated screen

However, it is obvious that in a short period of time through the process of absorption of infrared radiation, the metallic mesh sections lead to an increase in its temperature, which we can calculate with sufficient accuracy from the formula:

$$T = \sqrt[4]{\frac{Q_1}{\sigma} \frac{\alpha_m}{\epsilon_T}}, \quad Q_1 = \alpha_0 P_0 \tag{2}$$

Here α_m - absorption factor, absorption coefficient of IR-radiation for metals is determined by emissivity that is for unpolished

oxidized metallic surfaces in the range of 0.8-0.98, $\sigma = 5.6687 \times 10^{-8} \text{ W/(m}^2\text{K}^4)$ - the Stefan-Boltzmann constant, ε_t - emissivity for the unpolished oxidized steel surfaces in the temperature within 500 °K -1100 °K is between 0.78 - 0.87.

The amount of thermal radiation emitted to the grid in the absence of water-cooling heats the grid, and the hot grid becomes a secondary source of thermal radiation with luminosity defined by:

$$Q_E = \varepsilon_T \sigma (T^4 - T_1^4) \quad (3)$$

Where T_1 - ambient temperature; therefore, the heat flux density transmitted through the grid can be defined by the equation:

$$Q_s = (1 - \alpha) P_0 + Q_E \quad (4)$$

However, the secondary radiant heat flux depends on the temperature of the grid as well as on the mode of heat transfer at each individual element of the device Equation 3.

At the initial stage, both grids reduce the radiant heat flux $-P_0$ four times at absorption factor $\alpha_0 = 1/2$. Yet, as the grid becomes hot, it begins to transfer the heat that is known as a secondary source of thermal radiation. The sufficiently high values of $-P_0$ may result in the destruction of grids.

Nonetheless, immediate water supply in the system creates various modes of thermal protection. The flow rate is specified based on the degree of attenuation needed with regard to the value of heat exposure.

If the rate of water flow on the surface of the grid is less than the rate of evaporation, then it does not form the water film on the surface. Therefore, this case is a mode of "dry net". Otherwise, the water merging on the grid will form a continuous water film so-called a mode of "wet net".

In the case of "dry net" the water droplets that are produced by nozzle fully evaporate absorbing the heat flux as a result of the steady mode of a droplet heating from initial $T=20$ °C until boiling and then evaporation will occur caused by the temperature of the water and temperature on the grid. Thus, it is determined by:

$$DQ_1^c = \frac{V_1^c}{S_{eff}} [l + C_p (T_{100} - T_{20})] \quad (5)$$

Where: V_1^c - Water flow rate to the grid [kg/s];

S_{eff} - Surface area of the grid from which water evaporates [m²];

λ - Specific Heat of vaporization [kJ/Kg];

C_p - Specific heat capacity of water [J/ (kg * K)]

In the case of "wet net" expression (5) becomes:

$$\frac{V_1}{S_{S1}} (\lambda + c_p (T_{100} - T_0)) + \frac{V_{1P} m}{l h_{1P}} c_p (T_{1P} - T_0) \quad (6)$$

Where: V_1 - Rate of water evaporation on the grid surface

V_{1P} - Velocity of dripping water film ($V_1 + V_{1R} = V$),

h_{1P} - Thickness of the water film;

T_{1P} - Temperature of the water film determined by one-dimensional equation of thermal conductivity:

$$\frac{1}{\alpha} \frac{dT}{dt} = \frac{d^2T}{dx^2} \quad 0 < x < h, t > 0 \quad (7)$$

With boundary conditions:

$$k \frac{dT}{dx} \Big|_{x=0} = Q_{1E} - \eta_{1P} (T_{100} - T_0) + c_p V_{1P} (T_0 - T);$$

$$k \frac{dT}{dx} \Big|_{x=h} = -\eta_{PB} (T - T_0) + c_p V_{1B} (T_0 - T);$$

$$T|_{t=0} = T_0$$

Here: $Q_{1E} = \varepsilon_T \sigma (T_1^4 - T_0^4)$

T_1 - Temperature is determined by the formula (1) - $T_0 = 20$ °C;

η_{1P} - Constant heat exchange between the grid and the surface of water film;

η_{PB} - Constant heat transfer of outer surface of water film with the surrounding environment;

V_{1B} - Water flow rate to the outer surface of water film;

The theoretical expression of the second grid is derived using formulas similar to (6) and (7), as in the case of "wet net".

The absorption of radiant heat flux due to optical phenomena of scattering IR-radiation on water films that form on the grid is not considered in this study as well as the water droplets movements within the space between grids. In order to perform numerical calculations, the necessary parameters were obtained from experiments [26,27]. The numerical estimation of an absorption coefficient $-K$ was based on quantitative estimates of following studies: Average rate of water supply to the grid as well as the average speed of water droplets movement and the total number of droplets within the volume between two of the grids at a time.

The comparison of thermo-physical computation and experimental data for the two extreme cases when water consumption $-Q$ is up to 80 g/s for ("wet grid") and 38 g/s for ("dry grid") under maximum incident heat flux $-P_0$ Are shown in Table 2.

The theoretical values of the attenuation coefficient $-K$ vary due to the difference in the consumption of water. In the case of "wet net", the attenuation coefficient is 2.6 times greater than in the case of "dry net" when the difference in the consumption of water only 2 times. It is explained by the water discharge at a flow rate of 80 g/s that forms water films on the surface of the grid known as "wet net".

Table 2: Theoretical and Experimental values "K" for two grids at various water flow when the radiant heat exposure $P_0 = 22 \text{ kW/m}^2$

№ Condition	Water discharge, g/s	Attenuation coefficient "K"		Variation
		Theoretical value	Experimental data	
1. "Wet net"	80	88	130	30%
2. "Dry net"	38	33	40	18%

It should be noted that the experimental values of $-K$ for "wet net" condition were at least three times higher than the corresponding event of "dry net". Also, the variation between theoretical and experimental values of $-K$ in the case of "wet net" is almost two times higher than the corresponding case of "dry net". This suggests that the proposed simplified theoretical model more accurately describes the case of "dry net" while it takes into account only thermo-physical effects of the process of absorption that gives variation in "wet net" case.

One of the reasons for these variations is due to an approach to heat and mass transfer that has been considered separately for each element of the design. Another reason for the discrepancy between theoretical and experimental results is that this model does not fully address the optical effect that includes the scattering of radiation by water droplets. Also, an absence of the optical effect in the theoretical analysis of water film at the flow rate of 80 g/s or more provides the most

significant contribution to the difference between the theoretical and experimental data.

The complex theoretical and experimental study in this work allows interpretation of the above experimental data as follows: substantial changes on the value of $-K$ dependent on the amount of heat transfer exposed on-screen and the water supply rate as given in Table 1. It also changes by the effect of spectral selectivity in weakening electromagnetic radiation using heat screen "Sogda" [16].

The analysis of the experimental data shown in Table 1 indicates that the values for attenuation coefficient $-K$ do not change significantly for the "dry net" case (at a flow rate of 38 g/s) when exposure level of heat flux decreases, i.e., by increasing the distance $-R$ between the screen and radiant heat source. However, in the case of "wet net" at a flow rate of 80 g/s, the value for $-K$ rises significantly as distance $-R$ between the screen and radiant heat source increases. In term of the "dry net" condition, the variation in the experimental and theoretical studies can be

explained as follows: An aforementioned experimental data and thermal-physical computations are conducted without taking into account an optical phenomenon that adequately describes the physical process of absorption of the heat flux, regardless of it is the degree of heat flux. For the 2nd case, water film on the surface of the grid results in a sharp increase in the role of the optical effects of IR radiation on water films that are not included in our thermal-physical estimates. In this regard, it can be affirmed that the known dependence of geometric and dynamic parameters of disturbances on the surface of the water films is a cause of the viscosity and surface tension factor of water film, the values of which are highly dependent on the temperature of the water droplet environment. In this experiment, it indicates the significant rise in the value of the attenuation coefficient –“*K*” when the temperature of the water film is reduced from 85 °C at a radiant heat flux of 25 *kW/m²* to 17 °C at radiant heat of 4 *kW/m²*. The reduction in temperature –*T*, achieved by increasing the distance –*R* between the screen and radiant heat source is shown in Table 1.

Spectral selectivity in the degree of attenuation of short- and long-wavelength electromagnetic spectrum in the most common classes of fires is an important advantage of the heated screen "Sogda". In addition, it remains the semi-transparent in terms of visibility in a fire zone that enables firefighters to evaluate the risk in the fire scenario and make the necessary decision.

The formation of disturbances on the surface of water films (including surface waves) for the given geometric parameters is determined by the physical processes that are comparable with the wavelengths of IR-radiation in the most common classes of fires. In particular, the formation of such rivulet results in a strong increase of scattering in the processes of absorbing the IR-radiation that passes through the heated screen. However, these revolute with the geometric parameters that far exceed the diapason of wavelengths of visible light as the radiation from

a fire - short optical diapason cannot essentially influence the attenuation of visible light passing through a screen with a water film on the surface of the grid for optical processes. In the latter case, it was obvious that only the ratio between the total area of the grid and the lumen of the grid cells – α_0 , plays a role in reducing the visible portion of thermal radiation from a fire. The statistical size distribution of water droplets within the space between two grids, produced at a pressure of 0.4- 0.6 MPa, shows that they also do not leave a considerable impact on the process of visible light passing through a screen. This is due to the fact that the overwhelming portion of the water droplets is more than two orders greater than the wavelengths of the visible spectrum.

As discussed above, when $\alpha_0 = 0.5$ the half of radiant heat energy will not pass through the grid due to the most of it absorbed by the metal grid. The continuous water-cooling of the metal grid will prevent the further heat up, and the grid does not become a source of secondary radiant heat. Therefore, a dual grid surface in both cases creates a barrier for visibility that weakens it only four times resulting in a decrease of ten times or more in the attenuation coefficient of IR-spectrum of the radiation exposure.

A condition close to a real fire has been created to record the degree of attenuation of radiant heat flux that has exceeded the value of 25 *kW/m²*.

At the first stage, the fire load consisting of wooden railway sleepers as a fire source (stack size of 2m × 3m × 1.6 m), fire load –667 *kg/m²* was ignited that caused flame temperature to rise up to 1100 °C. The maximum value of radiant heat flux was 65 *kW/m²* at the distance *R*= 0.8 m from the source of a fire, and it was shown that only at a distance greater than 6 m radiant heat flow values fell to less than 4.2 *kW/m²*. It was recorded that when exposed to a radiant heat flux of 65 *Kw/m²* on one side of the screen, the radiant heat reduced to the value not exceeding 1 *kW/m²* ($k \sim 65$ times) on the other.

LNG experiment

The main objectives of developing these fire protection methods are to prevent the possible spread of steam and gas clouds during the emergency response, where spills of liquefied flammable gas occur in production facilities and cryogenic storage facilities. In emergency situations under the depressurized condition of production facilities, fire and explosive, toxic clouds formed as a result of intensive evaporation of spilled product (hazardous liquid) can spread over long distances. Ignition of this type of cloud is often accompanied by explosions, destructing technological communications, apparatus and vessels, the formation of new zones for further spills of the product as well as the generation of super-heat flow, which leads to the formation of new fire sources. Therefore, storage and use of LNG and methods of transportation will meet strict requirements to provide people with protection and production facilities. One of the most important problems of LNG consumption, especially at remote sites, is to ensure its safe storage in small surface vessels. Previously proposed methods and devices have a number of shortcomings and are not widely used [1,2].

The data of later experimental data is given (from 2010-2012 Orenburg, Russia) that devoted to the study of the quality of fire protection around cylindrical vessels with CPG. This construction allows for safe storage of highly flammable gases in the form of a leak-proof, fire-resistant structure, preventing the spread of fire and explosion in the case of a gas leak.

In 2010-2011, experimental studies were carried out in the Fire test centre of Russian Research Institute of Fire Protection (EMERCOM of Russia) in the Orenburg region, to study the application of innovative technology to provide fire and explosion safety for LNG storage facilities. A cylindrical vessel with a diameter of 1m of LNG and a height of 3m was placed in the centre of the concrete embankment (3m*3m*1m). Four screening panels (3m*4m*0,2m) were mounted

on the top edge of the embankment, forming a solid fence in the form of a rectangular shape.

In the second stage, the efficiency of heat screen was determined by placing it closer to burning Liquefied Natural Gas (LNG) storage. In the initial period of 1 min, the initiated pre-planned emergency spilled out of LNG inside the enclosure was allowed with no water supply to form water film within the grid. Therefore, after approximately 3-5s, the steamy gas started to easily spread through the bottom of the mesh fence panels and freely distributed on the ground surface. At the next stage, sealing water film was formed on the surface of the grid in the fence panels due to the activated water discharge at the fence panel. After evaporating, gas-filled the whole enclosure volume, the heavy gaseous clouds spread straight up and started to spread through the hole in the upper part of the fence, then scattering in the upper atmosphere. In the future, as shown in Figure 5, the design was improved, increasing the dissipation efficiency of gaseous clouds.



Figure 5: Experimental view of the spread of heavy gaseous clouds

When the burning gas evaporated within the fence, explosion pressure stress did not lead to structural failure, and the water film was instantly restored, retaining all the properties of the fence. Combustion gas inside the enclosure moved to the upper section of the fence due to

the lack of oxygen within the enclosure, see Figure 6.



Figure 6: Burning LNG surrounded by the protective fence "SOGDA"

Experimental studies were carried out with burning LNG with the protective fence to develop the Fire and Explosion safety for LNG storage facilities against the radiation heat flux from an external source. Measurement analysis of heat flux and flame temperature indicates the following: Flame temperature reached $T = 1800$ °C; Value of the radiant heat flux exposed on the screen was more than 220 kW/m^2 , and passing through it, the value of the heat flux was less than 4.8 kW/m^2 ($k \sim 45$ times).

Summary of Results

1. The experimental research through the developed test generated heat flow up to 25 kW/m^2 , resulting in the following findings:

- Optimization of the screen design revealed a sharp increase in an attenuation coefficient –“ K ” that was more than 100 times due to provided water flow rate up to 80 g/s to 1 m^2 screen, followed by the formation of water films on the grid surfaces. In this case, it was found that a further increase in water consumption did not significantly change the value of –“ K ” .
- Performance review of the screen under the various level of radiant heat exposure indicated that there was a significant difference in the values of attenuation coefficient –“ K ” at “wet grid’

mode. The variation was associated with the formation of water films on the surface of the screen that had a significant impact on scattering radiant heat flux. Screen performance also reduced the visible spectrum radiation of fire only a few times, remaining the screen translucent that enabled visibility for the situation in the zone of a fire that enabled firefighters to evaluate the risk to make operational decisions.

- Testing the performance of the screens in conditions close to real fire scenarios showed that they retained a high degree of attenuation of heat flux at heat fluxes much larger than those achieved throughout the experimental tests. In case of the combustion of solid materials (most often - wooden structure) when maximum heat flow did not exceed 70 kW/m^2 , the screens could absorb the heat flow by at least a factor of 65 ($k \sim 65$). In the case of LNG fire that gave the maximum values for heat fluxes over 220 kW/m^2 , the screens could weaken heat flow not less than 45 times ($k \sim 45$).

2. Experimental studies on the application of innovative technologies to protect LNG facilities using grid fences showed the following performance that could not be achieved in any other way:

- Fenced area when operating in the normal mode ventilated through the mesh surface, which prevented the accumulation of gas to explosive concentrations inside the enclosure with little technological leaks;
- When a gas leakage occurred, it automatically activated the water supply, creating a water film that made the fence of the enclosure impervious to steam and gas clouds. This led to the movement of the clouds only up, further scattering to safe concentrations and dispersing;
- In case of a fire outside of the shielding surface, the enclosing fence protected the LNG storage against heat flow from the outside and prevented dangerous overheating;
- In case of a fire inside the enclosure, protective fence surface prevented the spread of fire and provided extinguishment inside the

enclosure, restricting the oxygen through the grids of the fence;

- Gas explosion, vaporized inside the enclosure, did not lead to the destruction of fences: water film was destructed, and excess pressure was dropped. After balancing the pressure of the water film formed on the back of the grid surfaces, fences and all properties were preserved.

Conclusion

It should be noted that the obtained unique results of these experiments confirmed the possibility of the wide use of heat shields, as mentioned at the beginning of this article. Application in nuclear and chemical facilities provided protection from heat flow due to the water film formed on the surface of the grid. Also, the screens were intended to inhibit the flow of hot combustion products containing radionuclides and hazardous chemical active gases. The recent catastrophic events in nuclear power plants in Japan suggest the urgent need for various forms of a protective fence "Sogda" to address the issue by reducing the risk as low as reasonably practicable.

For indoor Petrol Stations or Hazardous Chemical plants, the protective fence design "Sogda" could be constructed to create protective evacuation corridors for occupants as well as for separation of space into separate compartments to prevent further spread of fire. During normal operation, the protective fence would fit well into the interior of the premises. Also, the protective fence allows sound and light to penetrate freely through its grid surface. In case of fire or accidental release of gases, water supply is provided automatically or manually to activate the water spray nozzle between the grid fence panels. The protective fence surface instantly becomes impervious to large enough heat flows, flows of hazardous gases and combustion gases containing radionuclides. Therefore, all the conditions for the safe evacuation of plant personnel and the prevention of a catastrophic accident could be provided. It also seemed

appropriate to explore the possibility of installing these fences around these dangerous buildings, at the very least to prevent the spread of dangerous gases into the environment.

Currently developed technology to protect LNG facilities with Grid fencing is at the stage of patenting in Uzbekistan, also filed an international application under the Patent Cooperation Treaty (PCT) with priority from 28.06.2011.

Conflict of Interest

We have no conflicts of interest to disclose.

References

- [1]. Azarm M.A., Travis R.J., *Fire Safety In Nuclear Power Plants: A Risk-Informed And Performance-Based Approach*. Brookhaven National Lab., Upton, NY (US), 1999
- [2]. Li J., Huang Z., *Procedia Eng.*, 2012, **45**:70
- [3]. Zhao J., Li W., Bai C., *Chem. Eng. Trans.*, 2017, **62**:1345
- [4]. Guide I.S., *Safety Series No NS-G-1.7 Protection against Internal Fires and Explosions in the Design of Nuclear Power Plants*. IAEA, 2004
- [5]. Beard A.N., Burke G., Finucane M.T. *Nucl. Eng. Des.*, 1991, **125**:367
- [6]. Simion G.P., VanHorn R.L., Smith C.L., Bickel J.H., Sattison M.B., Bulmahn K.D., *Risk analysis of highly combustible gas storage, supply, and distribution systems in PWR Plants* (No. NUREG/CR-5759; EGG-2640). Nuclear Regulatory Commission, Washington, DC (United States). Div. of Safety Issue Resolution; EG and G Idaho, Inc., Idaho Falls, ID (United States). 1993
- [7]. Roewekamp M., Berg H.P., SMiRT 23. 14th international seminar on fire safety in nuclear power plants and installations. Gesellschaft fuer Anlagen-und Reaktorsicherheit (GRS) gGmbH, 2015
- [8]. DiNunno P.J., *SFPE handbook of fire protection engineering*. 2008
- [9]. Berg H.P., Fritze N. J. *Konbin*, 2012, **23**:5
- [10]. Bruynooghe C., Bucalossi A., *Fire protection in NPP: Challenges posed by fires to the Structures*. Systems and Components of Nuclear Power

- Plants, Report n1EUR-23231 EN from the Joint Research Centre (European Commission), 2008
- [11]. Kisner R.A., Wilgen J.B., Ewing P.D., Korsah K., Antonescu C.E., *Regulatory guidance for lightning protection in nuclear power plants*. United States: American Nuclear Society-ANS. 2006
- [12]. Jiayu Z., Qiang S., Juan L., Zhiwei F., Wei S., Jiayun C., Chunming Z., Jianshe C., *Procedia Eng.*, 2012, **43**:318
- [13]. Lee B.T., *Heat release rate characteristics of some combustible fuel sources in Nuclear Power Plants (NBSIR 85-3195)*. Gaithersburg, MD: National Bureau of Standards, 1985
- [14]. Ramana M.V., Nayyar A.H., Schoeppner M., *Sci. Global Secur.*, 2016, **24**:174
- [15]. Asamoah, M., Díaz, P., Dies, J., de Blas, A., *J. Appl. Sci. Technol.*, 2019, **23**:10
- [16]. Wu Y., *Fire Compartment and Fire Barrier Evaluation in the NPP Fire PSA*. In International Conference Pacific Basin Nuclear Conference Springer, Singapore. 2016, 351
- [17]. Alem M., Teimouri A., Salavati H., Kazemi S., *Chem. Methodol.*, 2017, **1**: 49
- [18]. Ali-Asgari Dehaghi H.R., Jabbari H., Kalae M.R., Mazinani S., Taheri M., Sedaghat N., *Chem. Methodol.*, 2019, **3**:306
- [19]. Budykina T.A., Budykina K.Y., *RUDN J. Ecol. Life Safety*, 2017, **25**:132
- [20]. Dombrovsky L.A., Levashov V.Y., Kryukov A.P., Dembele S., Wen J.X., *Int. J. Therm. Sci.*, 2020, **152**:106299
- [21]. Chhabra A.K., Talukdar P., *Int. J. Numer. Method. H.*, 2019, **29**:146
- [22]. Acosta C.A., Bhalla A., Guo R., *Photonic Fiber and Crystal Devices: Advances in Materials and Innovations in Device Applications XIII*, International Society for Optics and Photonics, 2019, 11123: 111230Y
- [23]. Ezhov V.S., Semicheva N.E., Bredikhina N.V., Semerinov V.G., Ezhova T.V., *Chem. Pet. Eng.*, 2019, **55**:514
- [24]. Chernoiivanov V., Katkov A., Gabitov I., Yukhin G., Martynov V., Khasanov E., Mudarisov S., Baltikov D., Khammatov R., Kovalev P., *Bulg. J. Agric. Sci.*, 2019, **25**:45
- [25]. Gustafsson M., Schab K., Jelinek L., Capek M., *New J. Phys.*, 2020, **22**:073013
- [26]. Pustovalov V.K., *SN Appl. Sci.*, 2019, **1**:356
- [27]. Cheng Z., Shuai Y., Gong D., Wang F., Liang H., Li G., *Sci. China Technol. Sci.*, 2020, **3**:1

HOW TO CITE THIS ARTICLE

Abykanova B., Karatayeva K., Shazhdekeyeva N., Suleimenova B., Bekova G., Kochshanova G., Yerekeshova A., Urazgaliyeva M. A Novel Approach to Stop the Fire Spread, Hazardous Gases and Radionuclides, *Chem. Methodol.*, 2021, 4(2) 166-177

DOI: [10.22034/chemm.2021.122287](https://doi.org/10.22034/chemm.2021.122287)

URL: http://www.chemmethod.com/article_122287.html